Chapter 9
High Pressure NMR Methods for Characterizing Functional Substates of Proteins

Hans Robert Kalbitzer

Abstract Proteins usually exist in multiple conformational states in solution. High pressure NMR spectroscopy is a well-suited method to identify these states. In addition, these states can be characterized by their thermodynamic parameters, the free enthalpies at ambient pressure, the partial molar volumes, and the partial molar compressibility that can be obtained from the analysis of the high pressure NMR data. Two main types of states of proteins exist, functional states and folding states. There is a strong link between these two types, the functional states represent essential folding states (intermediates), other folding states may have no functional meaning (optional folding states). In this chapter, this concept is tested on the Ras protein, an important proto-oncogen in humans where all substates required by theory can be identified experimentally by high pressure NMR spectroscopy. Finally, we show how these data can be used to develop allosteric inhibitors of proteins.

Keywords Conformational states • Drug design • Essential folding intermediates • High pressure NMR spectroscopy • Ras

9.1 Overview

In solution, proteins are not rigid but exist in a multitude of different conformations. This conformational ensemble (typically $3 \cdot 10^{17}$ molecules in solution NMR spectroscopy) is usually visible in the NMR spectra. Therefore, a single lowest energy or crystal structure usually cannot describe the NMR spectra satisfactorily as we have shown for the chemical shifts of a protein data set. Here, the agreement between experimentally observed chemical shifts and chemical shifts recalculated from the structures increases with the number of structures used (Baskaran et al. 2010). Figure 9.1 shows the error ε of the calculated shifts for HPr (histidine

H.R. Kalbitzer (✉)
Institute of Biophysics and Physical Biochemistry, University of Regensburg, D-93040 Regensburg, Universitätsstr. 31, Germany
e-mail: Hans-Robert.Kalbitzer@biologie.uni-regensburg.de

K. Akasaka, H. Matsuki (eds.), *High Pressure Bioscience*,
Subcellular Biochemistry 72, DOI 10.1007/978-94-017-9918-8_9

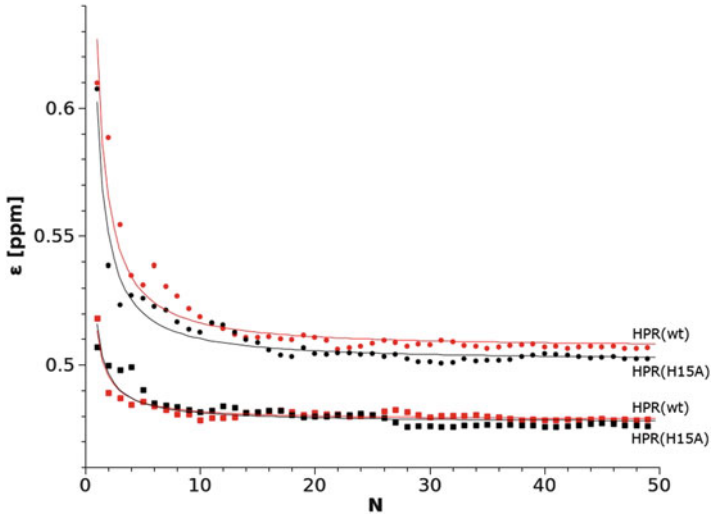

Fig. 9.1 Minimum ensemble size required for a prediction of the backbone chemical shifts. The mean chemical shift error ε of the backbone resonances is plotted as a function of the number N of structures used for the calculation of the backbone chemical shifts by the program SHIFTX (Neal et al. 2003). HPr-wild type (red) and HPr(H15A) (black) before (circle) and after (square) water refinement. The data were fitted with the lognormal function. $\varepsilon = \frac{1}{N\sigma\sqrt{2\pi}} e^{-\frac{(\ln\ N)^2}{2\sigma^2}} + C$ (Modified from Baskaran et al. (2010))

containing protein), a small protein from *Staphyloccocus aureus* as a function of the number of structures used for the calculations. The chemical shifts of different nuclei were weighted according to Schumann et al. (2007). HPr is a protein that probably occurs in a dominant main conformation that means in first approximation it can be represented by an ensemble of rapidly interconverting conformations with a single minimum of free energy. It turns out that for optimally representing the chemical shifts of the backbone atoms H, N, C^{α}, H^{α}, and C' 10–20 different structures are required. Refinement of the structures in explicit water results in some improvement, but does not remove the necessity of taking more than one structure (Fig. 9.1). Note that chemical shift calculations are not very accurate; there is still a remarkable systematic error in the calculation. Presently it is approximately 0.5 ppm, it seems possible that a higher accuracy of chemical shift calculation would increase substantially the number of structures required to reach an optimal prediction.

As we will see later, most probably for the majority of proteins more than one functional state exists; these (sub)states also have to be represented in the ensemble of structures by additional minima in the free energy landscape. The transition between these substates can be much slower than inside an ensemble that is part of a given substate. In this chapter we will focus on the application of high pressure

NMR spectroscopy for the elucidation of conformational equilibria of proteins that include a number of lowly occupied substates. In contrast to other methods it is possible by high pressure NMR spectroscopy to handle systems with multiple conformational states since it is possible to separate them on the basis of their pressure dependence and their specific thermodynamic parameters as their partial molar volumes and partial molar compressibilities.

9.2 Description of Pressure Effects in Multistate Systems

Most high pressure NMR experiments and also the experiments we discuss in the following are performed under equilibrium conditions and therefore can be described by classical equilibrium thermodynamics. If a protein occurs in N states i ($i = 1, \ldots, \mathrm{N}$), the populations p_i of the different states in thermodynamic equilibrium are determined by their differences in the free Gibbs energies ΔG_{ij} (Fig. 9.2) with

$$\frac{p_j}{p_i} = K_{ij} = \exp\left(-\frac{\Delta G_{ij}}{\mathrm{R}T}\right) \tag{9.1}$$

The equilibrium constant K_{ij} is dependent on pressure P and the absolute temperature T (R, gas constant). The pressure dependence of ΔG_{ij} at constant temperature T and hence of K_{ij} can be approximated by (Heremans and Smeller 1998)

$$\Delta G_{ij}(P) = \Delta G_{ij}^0(P_0) + \Delta V_{ij}^0(P - P_0) + \frac{1}{2}\frac{\partial \Delta V_{ij}^0}{\partial P}(P - P_0)^2 \tag{9.2}$$

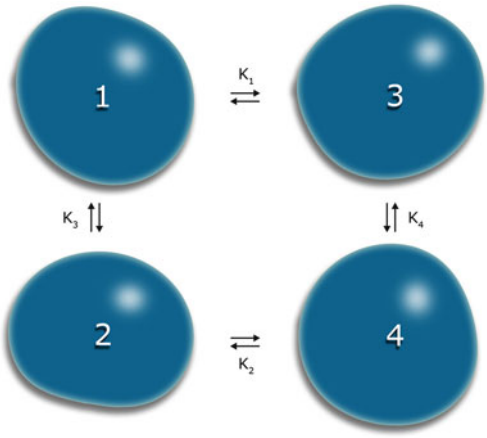

Fig. 9.2 Equilibrium between different conformational states in a four state model. $K_1 = [3]/[1]$, $K_2 = [4]/[2]$, $K_3 = [2]/[1]$, $K_4 = [4]/[3]$

The derivative in Eq. 9.2 is often abbreviated by

$$\Delta\beta_{ij}^{'0} = -\frac{\partial \Delta V_{ij}^{0}}{\partial P} \tag{9.3}$$

$\Delta G_{ij}{}^{0}$, and $\Delta V_{ij}{}^{0}$ are the differences of free energies and partial molar volumes, respectively, at temperature T_0 and pressure P_0.

The actual response observed in an NMR spectrum, strongly depends on the timescale of the exchange between the different states characterized by the exchange correlation times τ_{ij} and the differences of the respective parameters in the two states measured in frequency units. The parameter commonly evaluated in high pressure NMR spectroscopy is the chemical shift δ. Here the chemical shift difference $\Delta\omega_{ij}$ (measured in angular frequency units) between states i and j determines the NMR time scale. When the fast exchange condition $|\Delta\omega_{ij}\ \tau_{ij}| << 1$ holds for transitions between M^* states, then the correspondent chemical shifts are population averaged.

The chemical shift dependence of nucleus k on pressure is then given by (Baskaran et al. 2010)

$$\delta^k = \sum_{j=1}^{M*} p_j^* \delta_j^k = \frac{1}{Z*} \sum_{j=1}^{M*} \delta_j^k e^{\frac{-G_j}{RT}} = \frac{\sum_{i=1}^{M*} \delta_j^k e^{-\frac{\Delta G_{1j}}{RT}}}{\sum_{i=1}^{M*} e^{-\frac{\Delta G_{1j}}{RT}}} \tag{9.4}$$

For separating unspecific effects of pressure from the conformational effects of interest (Kremer et al. 2007) the chemical shifts can be corrected by subtracting the known pressure dependence of chemical shifts of the random-coil peptides such as Gly-Gly-Xxx-Ala or Ac-Gly-Gly-Xxx-Ala-NH_2 from the experimental data (Arnold et al. 2002; Koehler et al. 2012).

The size of the chemical shift changes is correlated to the size of the local conformational changes. Often the pressure dependence can be represented phenomenologically by the first and second order pressure coefficients B_1^* and B_2^* obtained from a Taylor expansion at the pressure P_0 and temperature T_0. The corrected chemical shifts δ^* are described by

$$\delta^*(P,\ T_0) = \delta_0^*(P_0,\ T_0) + B_1^*(P - P_0) + B_2^*(P - P_0)^2 \tag{9.5}$$

The pressure coefficients B_1^* and B_2^* can be interpreted in thermodynamic terms in a two-state system when the condition holds.

$$\left|\frac{\Delta G^0}{2RT}\right| << 1 \tag{9.6}$$

In this case the ratio of B_2^*/B_1^* is (Beck Erlach et al. 2014)

$$\frac{-2B_2^*}{B_1^*} = \frac{\Delta\beta'(P_0)}{\Delta V(P_0)} = <\beta^0> + <V^0> \frac{\Delta\beta^0}{\Delta V^0} \tag{9.7}$$

with the mean partial molar compressibility $<\beta> = <\beta'/V>$, the difference of the partial molar volumes and compressibilities ΔV and $\Delta\beta$, and the mean partial molar volumes $<V>$ of the two states. Note that the definition of B_2^* given by Beck Erlach et al. (2014) differs to that given in Eq. 9.5 by a factor of 2 taken into account in Eq. 9.7. For

$$\left|\frac{\Delta G^0}{2RT}\right| >> 1 \tag{9.8}$$

the following approximation holds

$$\frac{-2B_2^*}{B_1^*} = \frac{\Delta\beta'(P_0)}{\Delta V(P_0)} + \frac{\Delta V(P_0)}{RT_0} = <\beta^0> + <V^0> \frac{\Delta\beta^0}{\Delta V^0} + \frac{\Delta V^0}{RT_0} \tag{9.9}$$

When the conformational exchange between the states i and j is slow relative to the time scale of the NMR experiment ($|\Delta\omega_{ij}| >> 1/\tau_{ex}$), the signal volume V_i of state i is proportional to its concentration c_i. The equilibrium constant K_{ij} can be calculated from the cross peak volumes V of the HSQC spectra by

$$K_{ij} = \frac{V_j}{V_i} = e^{-\frac{\Delta G_{ij}}{RT}} \tag{9.10}$$

If only one peak i can be observed then V_i is given by

$$V_i(P) = \frac{V_T(P)}{\sum_{j=1}^{N} e^{-\frac{\Delta G_{ij}}{RT}}} \tag{9.11}$$

With $V_T(P)$ the total cross peak volume corresponding to the sum of all states at pressure P.

The relative population p_j of a state j in an N-state system can be calculated from the equilibrium constants $K_{ij} = [j]/[i]$ as

$$p_j(P, T_0) = \frac{K_{ij}(P, T_0)}{\sum_{j=1}^{N} K_{ij}(P, T_0)} \tag{9.12}$$

with i an arbitrarily selected state.

9.3 Ras-Dependent Signal Transduction

Proteins that interact with different partners are typical candidates for a multistate equilibrium. An excellent example of such a protein is the rat sarcoma (Ras) protein, a small guanine nucleotide binding protein that is involved in multiple signal transduction pathways that control cellular proliferation, differentiation, and apoptosis. It represents a kind of molecular switch, in its "off" state GDP is bound in its active center, in its "on" state GDP is replaced by GTP and the signal transmission is activated. Ras is activated by guanine nucleotide exchange factors (GEFs) and is deactivated by GTPase activating proteins (GAPs) (Fig. 9.3). Only in the GTP-bound state effector proteins bind to Ras with high affinity (Wittinghofer and Waldmann 2000; Herrmann 2003; Wennerberg et al. 2005; Rajalingam et al. 2007). Mutations of Ras that lead to a permanent activation of the Ras pathway are found in more than 30 % of all human tumors (Bos 1989; Karnoub and Weinberg 2008; Baines et al. 2011). Inhibiting the activity of Ras thus represents an interesting strategy in cancer therapy (for reviews see e.g. Adjei 2001; Friday and Adjei 2005; Baines et al. 2011).

When the Ras activation cycle (Fig. 9.3) is described by a multistate equilibrium, activated Ras with GTP bound has at least three different states, the GEF-interacting state 1(T), the effector binding state 2(T), and the GAP interacting state 3(T). Corresponding states for GDP can be defined when GDP is bound, however an interacting partner has not known for state 2(D). In addition, two states 1(0) and 3(0) are required where in state 1(0) the active centre is not occupied by a nucleotide and where in state 3(0) P_i is not yet released after GTP-hydrolysis (Fig. 9.3).

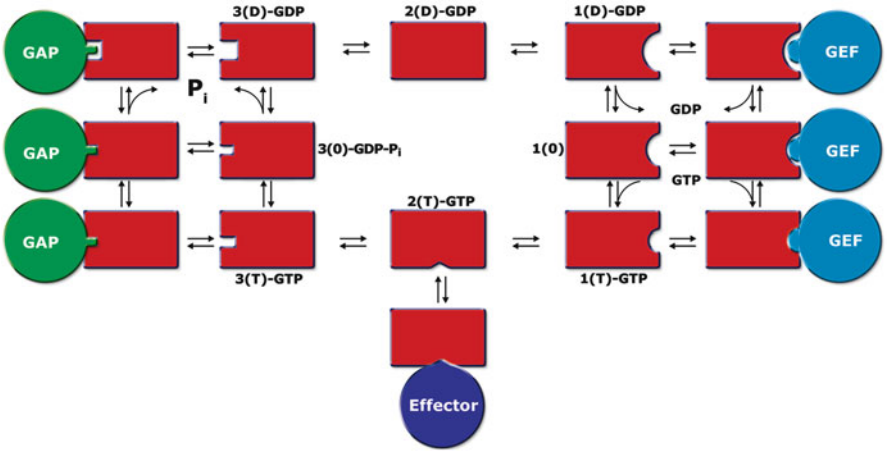

Fig. 9.3 Generalized Ras activation cycle. Ras, rat sarcoma protein, GAP, GTPase activating protein, GEF, guanine nucleotide exchange factor. 0, D, and T designate the nucleotide-free or GDP-Pi containing, the GDP bound, and the GTP bound state of the Ras protein (Modified from Kalbitzer et al. (2013a))

9.4 A Fundamental Link Between Functional States and Folding Intermediates

An important application of high pressure NMR spectroscopy is the investigation of folding/unfolding of proteins and the detection of folding intermediates. Classically, folding studies and functional studies are two separate areas that are dealt with by different groups of scientists. However, when considering the two processes in the light of the free energy landscape model it becomes evident that there is a fundamental link between folding and function (Kalbitzer et al. 2009). In thermodynamic equilibrium all energetically possible states become populated and are accessible; the same free energy landscape describes folding and function. Only the transient populations of the different states (local free energy minima) after a perturbation depend on the selected initial conditions. To show the connection between the two domains we performed high pressure studies as well as classical denaturation studies with the Ras protein.

By ^{31}P NMR spectroscopy of Ras protein complexed with the non-hydrolysable GTP analog GppNHp two structural states of the protein can be identified, since the resonance lines of the γ- as well as the α-phosphate groups are split (Fig. 9.4). The integration of the peak areas gives the corresponding populations of the states. At low temperature the transitions between the two states are slow on the NMR time scale ($\tau_{ex} = 7.7$ ms) (Geyer et al. 1996). The functional importance of the two states was determined by adding GTPase activating proteins, effectors or exchange factors to a solution of Ras. Addition of effectors leads to the increase of one set of upfield shifted resonance lines, addition of the exchange factor SOS (son

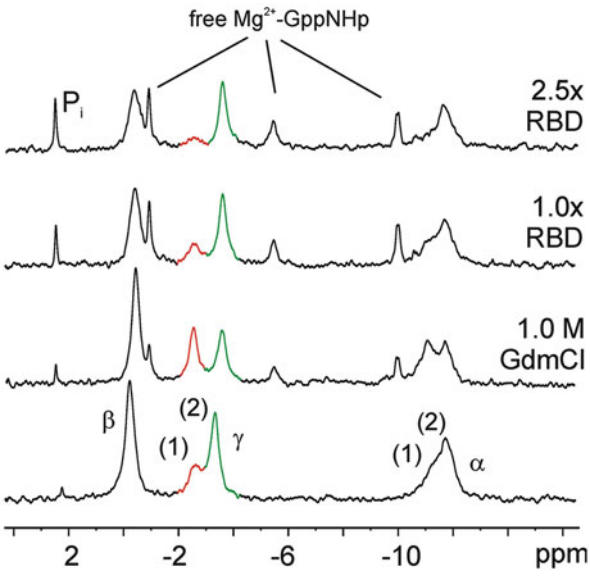

Fig. 9.4 Denaturation of Ras complexed with Mg^{2+}·GppNHp studied by ^{31}P NMR spectroscopy. ^{31}P NMR spectrum of Ras·Mg^{2+}·GppNHp changes after successive addition of Guanidinium hydrochloride (GdmCl) and the Ras binding domain (RBD) of Raf kinase. α, β, and γ, signals of the α-, β-, and γ-phosphate group of the nucleotide. (1) and (2), Ras in state 1(T) and 2(T) (modified from Kalbitzer et al. (2009)). Temperature 278 K, ^{31}P resonance frequency 202.4 MHz

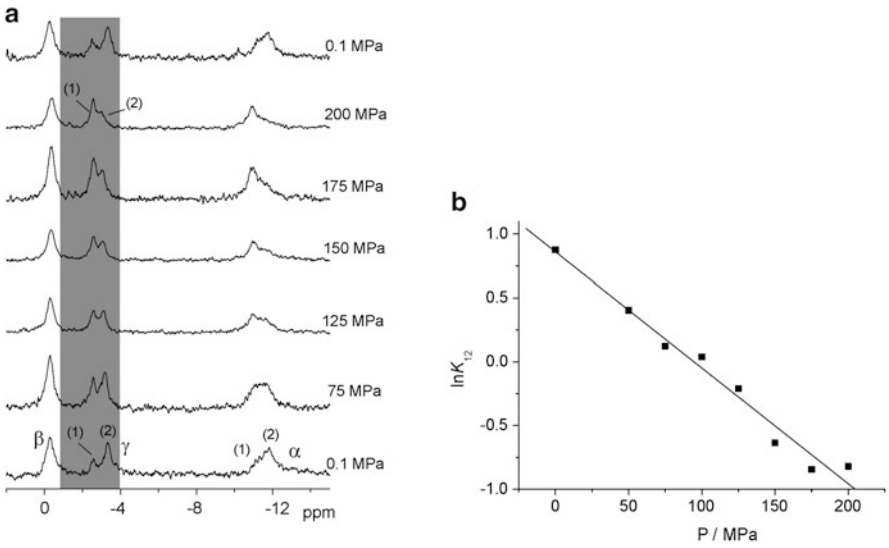

Fig. 9.5 ^{31}P NMR spectroscopy of Ras complexed with Mg^{2+}·GppNHp at different pressures. (**a**) ^{31}P NMR spectra of Ras·Mg^{2+}·GppNHp at different pressures. α, β, and γ, signals of the α-, β-, and γ-phosphate group of the nucleotide. (1) and (2), Ras in state 1(T) and 2(T). (**b**) Plot of ln $K = [2(T)]/[1(T)]$ as a function of pressure P. Temperature 278 K, ^{31}P resonance frequency 202.4 MHz. Difference of the free energy $\Delta G_{21}{}^0$ and the partial molar volume $\Delta V_{21}{}^0$ 1.42 kJ mol^{-1} and −17.2 mL mol^{-1} (Modified from Kalbitzer et al. (2009))

of sevenless) to an increase of the other set of downfield shifted resonance lines (Geyer et al. 1996; Spoerner et al. 2001; Kalbitzer et al. 2009). This means that after binding the population of the corresponding states 1(T) or 2(T) increases (Fig. 9.4). The equilibrium constant between the two states K_{12} is 1.9 at 278 K for the wild type protein (Spoerner et al. 2004) that corresponds to a difference of free energies $\Delta G_{12}{}^0$ of −1.5 kJ mol^{-1}. Applying pressure to the sample (Fig. 9.5a) leads to a shift of the equilibrium to the state with the smaller partial volume, in our case to state 1(T). A fit of ln K_{12} as function of the pressure P leads to a difference of the partial molar volumes ΔV_{12} of −17.2 mL mol^{-1}. According to the above suppositions, in classical denaturation experiments with a denaturant such as guanidininum hydrochloride (GdmCl) a shift of the equilibrium of the functional states should also be observed during the denaturation process. Figure 9.4 shows that this prediction is true, at 1 M GdmCl, the relative occupancy of state 1(T) is strongly increased and simultaneously some GppNHp is set free indicating beginning denaturation of the protein. As required from theory the population of state 1(T) is shifted again to the effector binding state 2(T) when the effector-binding domain (RBD) of the Raf kinase is added.

Thus the following paradigm can be formulated: the minimum number of folding intermediates is determined by the number of all required functional states of a protein ("essential" folding intermediates). Additional "optional folding" intermediates

may be observable (Kalbitzer et al. 2009). The main difference between the two perturbations of the equilibrium applied here (and also other perturbations such as temperature changes) is the observation, that the pressure perturbation usually separates the different states much better than the other perturbations. In addition, protein aggregation and virtually irreversible protein aggregation is suppressed at high pressures.

9.5 Conformational States of the Ras Protein Identified by High Pressure NMR Spectroscopy

When we describe protein-protein and protein-ligand interaction in the Monod-Wyman-Changeux model (Monod et al. 1965), different conformational substates of a protein with different affinities for the interaction partners are required. For the Ras protein, such a minimal scheme has been already introduced in Fig. 9.3. A possibility to detect these substates is the analysis of the high pressure NMR data that we recorded for the Ras protein with the GTP analog GppNHp bound. Figure 9.6 shows a superposition of HSQC-spectra of uniformly ^{15}N-enriched Ras protein recorded at different pressures in the range from 3 to 180 MPa. The signals of the backbone amide groups shift continuously with pressure, most of them in downfield direction. The pressure dependence of the chemical shift varies from amide group to amide group. In addition, some cross peak intensities are influenced by pressure and a few new cross peaks appear in the spectra at high pressures.

A first analysis of the size of the chemical shift changes was performed using the Taylor expansion described in Eq. 9.5. Before calculating the pressure coefficients,

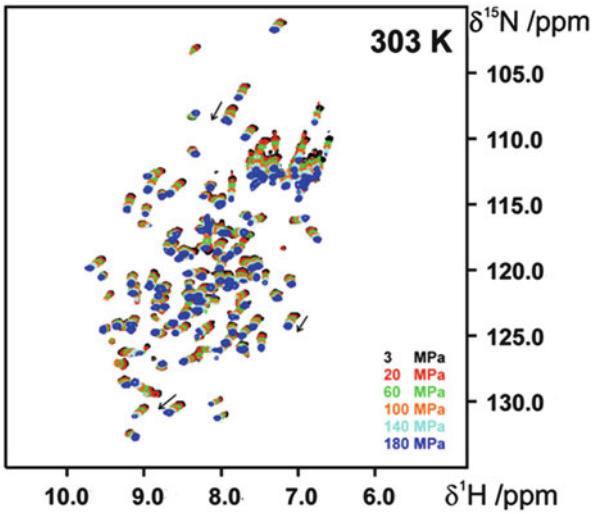

Fig. 9.6 [^{1}H,^{15}N]-HSQC spectra of Ras·Mg^{2+}·GppNHp at different pressures. Temperature 278 K. Proton resonance frequency 800.2 MHz (Modified from Kalbitzer et al. (2013a))

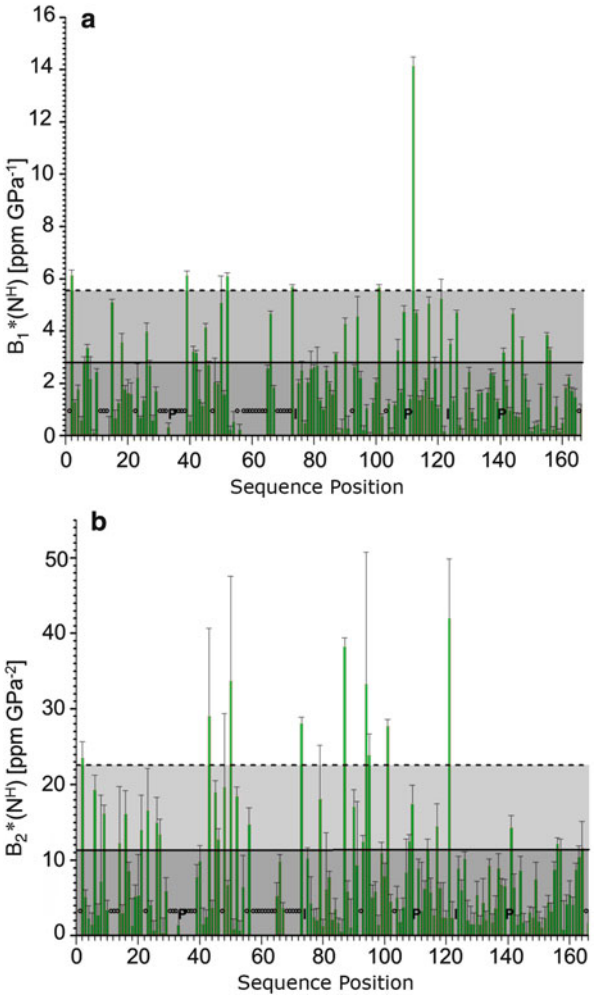

Fig. 9.7 Pressure induced chemical shift changes in wild type Ras·Mg^{2+} · GppNHp at 303 K. The absolute values of the first order and second order pressure coefficients B_1*(N^H) and B_2*(N^H) of the amide nitrogen shifts are plotted as a function of the position in amino acid sequence. Data were corrected for random coil effects before calculation of the pressure coefficients $B_{1,2}$*. Solid line, standard deviation σ_0 to zero, dashed line 2 σ_0. P, prolines; o, not assigned residues; I, residues for which the coefficients could not be determined due to the loss of signal intensity within the pressure series (Modified from Kalbitzer et al. (2013))

the random-coil pressure coefficients were subtracted for removing trivial pressure effects. The ^{1}H and ^{15}N first and second order pressure coefficients B_1* and B_2* were plotted on the surface of the crystal structure of Ras·Mg^{2+}·GppNHp (Pai et al. 1990). In this crystal structure only the structure of Ras in state 2(T) could be detected although ^{31}P solid state NMR experiments have revealed that the single crystals used for the X-ray structure determination also simultaneously contain molecules in state 1(T) (Stumber et al. 2002; Iuga et al. 2004). In Fig. 9.7 the absolute values of the nitrogen first and second order pressure coefficients B_1* and B_2* are shown. For a number of residues values larger than the standard deviation to zero σ_0 are visible representing residues that are strongly influenced by pressure. The pressure effects are not restricted to the switch I and switch II regions but are also visible at the backside of the protein. The largest effects are observed

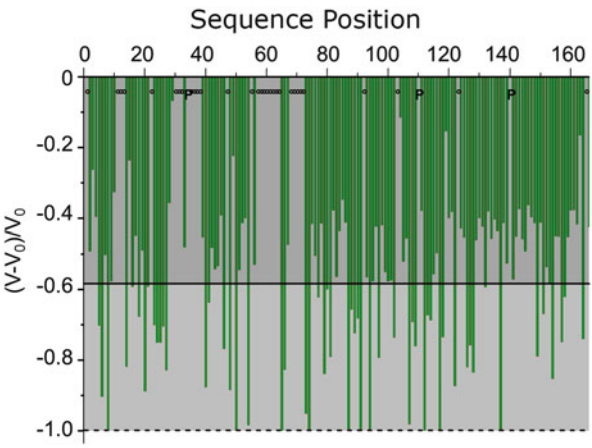

Fig. 9.8 Pressure-induced cross peak volume changes. Plot of the relative change of the [^{1}H, ^{15}N]-HSQC cross peak volumes V_0 measured at 3 MPa and V measured at 180 MPa. Temperature 303 K, solid line, standard deviation to zero σ_0

for Thr2, Ser39, Gln43, Thr50, Leu53, Ser65, Arg73, Thr87, His84, His94, Glu95, Ala121, Tyr141, and Lys147. Unfortunately, most of the residues in the switch regions are not visible in the [^{1}H,^{15}N]-HSQC spectra, meaning that pressure effects of these residues are not observable. However, Ser39 is located in switch I, Ser65 and Arg73 in the switch II region, indicating that these regions involved in protein-protein interactions probably are strongly influenced by pressure. Lys147 is part of the G3 motif that recognizes the guanine base of GTP.

In addition to chemical shift changes also position specific changes of the cross peak volumes can be observed. Strong cross peak volume changes usually are observed when slow exchange conditions apply. Typically, a cross peak assignable to the dominant state at ambient pressure loses intensity when at higher pressures the population of this state is reduced. A new cross peak corresponding to the high pressure state is to be expected. Such a peak often cannot be identified since it overlaps with other peaks or simply because it has not been assigned. Figure 9.8 shows the cross peak reductions at 180 MPa, the highest pressure used at 303 K. Again significant pressure effects are observable. Most of these residues influenced by pressure are located close to regions where large pressure dependent chemical shift changes occur.

The above analysis mainly describes the magnitude of the pressure-induced changes and gives only partial information on the mechanisms behind the observed changes. However, as a rule large second order terms B_2^* often are associated with larger conformational changes in the neighbourhood of the corresponding residue. In contrast, a thermodynamic analysis of the pressure-induced changes of NMR parameters such as chemical shifts or cross peak volumes gives information on the free energies and differences in the partial molar volumes of different states. Although the analysis is primarily restricted to the local probes such as the amide protons, identical structural transitions should also be characterized by a set of free energy differences ΔG^0, partial molar volume differences ΔV^0, and differences of the compressibility coefficients $\Delta\beta'^0$ measured at a temperature T_0 and a pressure

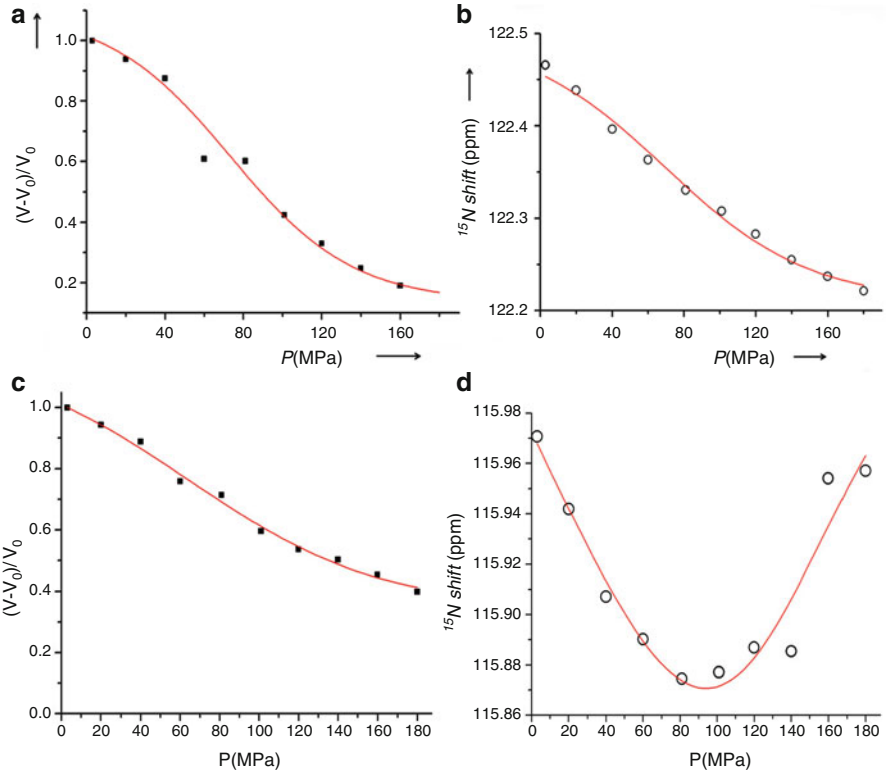

Fig. 9.9 Pressure dependence of ^{15}N chemical shifts and amide cross peak volumes in [^{1}H, ^{15}N]-HSQC spectra of Ras(wt)·Mg^{2+}·GppNHp. Temperature 303 K. Fit of the chemical shift changes (Eq. 9.5) and the normalized pressure dependent volume changes (Eq. 9.7). (**a**) Fit of the volume changes of Ala18, (**b**) fit of the chemical shift changes of Glu49, (**c**) fit of the volumes changes of Glu49. Data can be fitted with the same values for ΔG_{24} (12.4 kJ mol^{-1}), and ΔV_{24} ($-$115 mL mol^{-1}). (**d**) Fit of the chemical shift changes of Glu99, fit with a three-state model, ΔG_{21} 1.48 kJ mol^{-1}, ΔV_{21} $-$18 mL mol^{-1}, ΔG_{23} 5.2 kJ mol^{-1}, ΔV_{23} $-$81 mL mol^{-1} (from Kalbitzer et al. (2013))

P_0. Conversely, if similar thermodynamic parameters (identical within limits of error) are found for different residues, it is likely (but not mandatory) that these residues are involved in the same transition. A point making the analysis more difficult is the effect that in principle all residues are influenced by all transitions but to a different extent.

We have evaluated the high pressure induced chemical shift changes and cross peak volume changes of Ras·Mg^{2+}·GppNHp at two different temperatures, 278 and 303 K. For a satisfactory fit of the data (at least) four different states were required. In Fig. 9.9 some examples of such a fit are depicted. Biphasic curves such as shown in Fig. 9.9d can only be fitted when assuming at least three different states. Although the individual fit of different resonance lines does not give identical fit parameters because of the limited precision of the data, the obtained ΔG^0 and ΔV^0 values can be

Table 9.1 Conformational transitions and corresponding molar free energies ΔG^0 and molar volumes ΔV^0 of Ras(wt)·Mg^{2+}·GppNHp at 303 K[a]

Transition	K^0at 0.1 MPa	ΔG^0[kJ mol^{-1}]	ΔV^0[mL mol^{-1}]
2(T) → 1(T)	0.55	1.5 ± 0.2	−18 ± 1
2(T) → 3(T)	0.13	5.2 ± 0.3	−81 ± 3
2(T) → 1(0)	0.007	12.4 ± 0.4	−115 ± 2
1(T) → 1(0)	0.013	10.9 ± 0.3	−97 ± 2
1(T) → 1(0)[b]	0.03[b]	8.3[b]	
2(T) → 1(0)[b]	0.01[b]	9.8[b]	

[a]Values for $T = 303$ K. Within the limits of error the differences in free energies ΔG^0 and partial molar volumes ΔV^0 for the transitions 2(T) → 1(T) and 2(T) → 3(T) are independent of temperature in the range between 278 K and 303 K. ΔG^0 and ΔV^0 were determined from the pressure dependence of chemical shifts and cross peak volumes (data from Kalbitzer et al. 2013)
[b]Values from Kalbitzer et al. (2009) obtained at 278 K from a denaturation study with GdmCl. ΔG^0 was determined from the release of the nucleotide and interpreted as denaturation

grouped in the assumed three groups with overlapping error ranges. The obtained mean values of ΔG^0 and ΔV^0 then can be used for a satisfactory fit of all data corresponding to a given transition. That is shown in Fig. 9.9a, b where the same parameter set can be used to fit the pressure dependent ^{15}N chemical shift changes of Ala18 and the cross peak volume changes of Glu49.

The obtained parameters are summarized in Table 9.1. In this Table, the probable assignment of the transitions is already indicated, although that is by no means trivial. Only the assignment of the transition between state 2(T) to 1(T) is straightforward since this transition is already functionally defined by the ^{31}P NMR experiments that showed that one of the states (2(T)) interacts with effector proteins, the other state (1(T)) with the exchange factor SOS. The corresponding difference of the free energy $\Delta G_{21}{}^0$ and the partial molar volume $\Delta V_{21}{}^0$ obtained from the fit of the ^{31}P NMR data (Kalbitzer et al. 2009) were 1.42 kJ mol^{-1} and −17.2 mL mol^{-1} (see Fig. 9.5). Within the limits of error these values are identical to the corresponding values obtained from the analysis of the HSQC spectra for the 2(T) to 1(T) transition (Table 9.1).

Actually, the assignment of the other transitions in the proposed model (Fig. 9.3) can only be made on the basis of functional and structural properties. It is expected (and experimentally observed for Ras-mutants) that at very high pressures the nucleotide is released as it should occur in state 1(0). In fact, such a release of the nucleotide is also observed in denaturation studies of Ras with GdmCl (Kalbitzer et al. 2009). From this study also two ΔG^0 values are obtained for the transitions of 1(T) and 2(T) to 1(0) (Table 9.1). Taken into account that this study was performed at a different temperature, there is a good agreement between these values and the ΔG^0 values obtained from the analysis of the two-dimensional HSQC spectra. By exclusion, the third transition then can be associated with the 2(T) to 3(T) transition (Table 9.2). These assignments to the different transitions can be confirmed also by a structural analysis (see below).

Table 9.2 Populations of the different conformational states in Ras·Mg^{2+}·GppNHp.[a]

State i	p_i at 0.1 MPa
1(T)	0.326
2(T)	0.593
3(T)	0.077
1(0)	0.004

[a]The populations p_i were calculated with Eq. 9.12 from the equilibrium constants given in Table 9.1. Temperature 303 K, pressure 0.1 MPa

From the obtained free energies and partial molar volume differences it is possible to calculate the relative populations of the different states at any pressure. For practical purposes, the populations at ambient pressure are the most important (Table 9.2). The relative populations of state 1(T) and 2(T) are with 33 % and 59 % rather high and therefore they can be easily detected by ^{31}P NMR spectroscopy at ambient pressure. However, since the populations of states 3(T) and 1(0) are only 8 % and 0.4 %, they are almost undetectable by ^{31}P NMR. However, addition of GAP to a sample of Ras·Mg^{2+}·GppNHp leads to the growth of a new γ-phosphate peak (Geyer et al. 1996) at −3.0 ppm located just between the γ-phosphate resonances of state 1(T) and 2(T) at −2.6 and −3.3 ppm. If this would be the position of the γ-phosphate resonance of state 3(T), it could explain that the resonances of state 1(T) and 2(T) are not completely separated but show a kind of weak shoulder. A peak with a relative intensity smaller than 1 % as estimated for state 1(0) would disappear in the noise of the phosphorous resonance spectra.

It seems natural to assume that state 3(T), the interaction state with the GTPase activating protein GAP, has the highest intrinsic hydrolysis rate. Since in the reaction scheme (Fig. 9.3) state 2(T) is the direct neighbour of 3(T), it should also have a higher intrinsic hydrolysis activity than state 1(T). Experimental results support this assertion: the intrinsic hydrolysis rate increases when the population of state 2(T) is increased by site specific mutations or by effector binding stabilizing state 2(T) (Spoerner et al. 2010). An important point to have in mind when discussing the populations of the different states quantitatively is the dependence of the occupancy of the different states on the nucleotide analog used. Replacing the nucleotide analog GppNHp by the analog $GppCH_2p$ leads only to a small shift of the ratio of the populations K_{12} of state 2(T) to state 1(T) from 1.9 to 2.0 (Spoerner et al. 2005a). However, binding of the GTP analog GTPγS or the natural nucleotide GTP causes a dramatic decrease of the occupancy of state 1(T) with $K_{12} > 10$ (Spoerner et al. 2007) and $K_{12} > 20$ (Spoerner et al. 2010), respectively. Also C-terminal truncation after amino acid 166 influences the equilibrium between the two states and leads to a decrease of K_{12} for GTP to 11.3.

A powerful NMR method that provides complementary dynamical information in a multiple state system is the chemical exchange saturation transfer (CEST) spectroscopy. Essentially, a resonance line of a nucleus i in a conformational state a of a protein with a resonance position δ^i_a (that can be too weak to be observable in the spectrum) is saturated by a long, frequency selective weak pulse and the

saturation is transferred to the same resonance in conformational state *b* with a chemical shift δ^i_b. When the frequency of the saturation pulse is scanned through the spectral range, a decrease of the intensity of the resonance at position δ^i_b is observed when the saturation pulse hits the frequency position δ^i_a. This method has been introduced originally by Forsén and Hoffman (1963) in 1D-spectroscopy and has later been applied to identify the very weak ^{31}P resonance of GTP bound to Ras (Spoerner et al. 2010). An analysis of the data also gives the exchange rate between the two states as 7 s^{-1}. It can also be used in 2D spectroscopy e.g. [^{1}H, ^{15}N]-HSQC spectroscopy by introducing a long frequency selective ^{15}N pulse in the standard pulse sequence. Again, in the 2D-spectra cross peaks can be identified that are involved in chemical exchange. Surprisingly, its application to *H*-Ras(1–171)·Mg^{2+}·GTP led to an exchange rate that is with 72.3 s^{-1} almost one order of magnitude larger (Long et al. 2013). One reason could be that the CEST-experiment did not identify the correct transition since detailed state information is not available from CEST experiments.

An alternative method that is also able to obtain information about exchange processes and thus the existence of more than one conformational state are CPMG relaxation dispersion measurements (Loria et al. 1999) that where applied to *H*-Ras(1–171)·Mg^{2+}·GppNHp by O'Connor and Kovrigin (2008). However, it is not usable when the population of one state is extremely low as in the case of the GTP complex.

9.6 Drug-Design and High Pressure NMR Spectroscopy

Permanent activation of the Ras pathway leads to cell proliferation, a hallmark of tumor development. Looking at the scheme presented in Fig. 9.3 it is obvious that a new type of allosteric inhibition we call intrinsic allosteric inhibition is feasible and is in principle applicable to all proteins involved in signal transduction pathways (Kalbitzer et al. 2013; Kalbitzer and Spoerner 2013). It is obvious that the exclusive stabilization of one of the many structural states by selective binding of a small compound to that state will also modify the populations of all other states and thus the activity linked to them. For this mechanism it is not required that the small ligand binds on the interaction site of another protein such as the effector protein but it has to bind state selective. We have already shown that this mechanism is working since Zn^{2+}-cyclen binds selectively to Ras·Mg^{2+}·GppNHp in state 1(T), the weak effector binding state (Spoerner et al. 2005b). As to be expected the effector Raf has a substantially reduced affinity to activated Ras in the presence of this compound (Rosnizeck et al. 2010). Chemical shift perturbation studies reveal that this compound binds to the γ-phosphate of the bound nucleotide inside the nucleotide-binding pocket. Shortly after that we found a different compound, Zn^{2+}-BPA (bis(2-picloly)amine), that binds at a different position outside the active center but nevertheless mainly recognizes state 1(T). Again it suppresses the effector interaction (Rosnizeck et al. 2012).

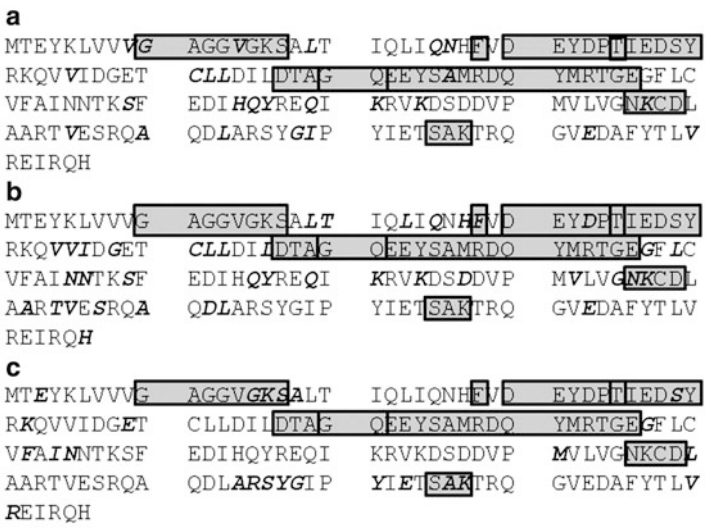

Fig. 9.10 Residues involved in different transitions in Ras. Grey areas correspond to known motifs, P-loop, PM1 motif (G10xxxxGKS17), G1-motif (F28), switch I (30–40), PM2 (T35), PM3 (D57xxGQ), switch II (60–76), G2-motif (N116KxD), G3 motif, (S145AK147). Highlighted are the residues involved in (**a**) the 2(T)-1(T) transition, in (**b**) the 2(T)-3(T) transition, and (**c**) in the 2(T)-1(0) transition (see Kalbitzer et al. 2013)

The question arises how to identify possible state specific binding sites. Here, an analysis of the high pressure response of the protein may help since residues can be identified that are predominantly influenced by a given transition. We have plotted the residues that are mainly influenced by a given transition as function of the position in the amino acid sequence (Fig. 9.10). In addition, the known structural and functional motifs are also indicated in Fig. 9.10. The residues sensible to pressure are located in known functional regions such as switch I and switch II as well as outside these regions. Another example is the 2(T) to 1(0) transition that is the transition to the nucleotide release state. It is also visible in the G3-motif (S145, A146, K147) known to be involved in an interaction of the base of the nucleotide.

Meanwhile, a number of small compounds have been published that either inhibit the effector binding or they influence the GEF-assisted nucleotide exchange. For Zn^{2+}-cyclen and Zn^{2+}-BPA we have shown that they stabilize state 1(T) but also lead to an increase of the population of state 1(0). Zn^{2+}-cyclen interacts with Gly12, Asp33, Thr35, and Ala59; unfortunately all these residues except Asp33 are not visible in the NMR-spectra of wild type Ras·Mg^{2+}·GppNHp. From the residues binding Zn^{2+}-BPA (Asp38, Ser39, Tyr40), only Ser39 is primarily influenced by the 2(T) to 1(0) transition.

Small molecules that inhibit the GDP to GTP exchange by the guanidine nucleotide exchange factor SOS were reported by several groups. One of them was DCAI (4,6-dichloro-2-methyl-3-aminoethyl-indole) interacting with Lys5, Leu6,

Val7, Ile55, Leu56, and Thr74 in Ras·Mg^{2+}·GDP (Maurer et al. 2012). None of these residues could be identified in Ras·Mg^{2+}·GppNHp as selectively influenced by a 2(T) to 1(T) or 2(T) to 1(0) transition. However, with Asp3, Cys51, Leu52, and Ile53 residues close to the interacting residues Lys5, Leu6, Val7, Ile55, and Leu56 are identified by high pressure NMR spectroscopy that are selective for the 1(0) and 1(T) state in Ras·Mg^{2+}·GppNHp, respectively. However, primarily a very close agreement is not to be expected since for the compound only the binding to the GDP state has been studied. Benzimidazole was reported to have similar effects by Maurer et al. (2012). Here, we could show experimentally by ^{31}P NMR spectroscopy that it induces a shift to state 1(T) when the GTP analog GppNHp is bound and thus stabilizes also a SOS binding state in triphospho nucleoside bound state (Kalbitzer et al. 2013; Kalbitzer and Spoerner 2013).

Sun et al. (2012) reported the SOS-inhibitor 2-((1*H*-Indol-3-yl)methyl)-3*H*-imidazo[4,5-*c*]pyridine that interacts with Lys5, Val7, Ser39, Asp54, Leu56, Tyr71, Thr74. Ser39 is characteristic for state 1(0), the nucleotide free state (Fig. 9.1) that could be permanently stabilized by SOS binding and thus could inhibit the nucleotide exchange. Also Lys5 and Val7 are close to Asp3 that selectively reacts in the transition to the nucleotide-free state 1(0) of Ras. Bisphenol introduced by Schöpel et al. (2013) as SOS inhibitor recognizes essentially the same binding pocket as the inhibitors described above.

9.7 Summary

To summarize, high pressure NMR spectroscopy provides the possibility to observe different conformational states of a protein that are involved in function or folding. Both processes are intimately linked together as derived from the free energy landscape model. For an analysis of the high pressure data it is necessary to carefully observe chemical shift and cross peak volume changes and to evaluate them with an appropriate model. The obtained data can be used to devise state specific inhibitors of functional proteins.

References

Adjei AA (2001) Blocking oncogenic Ras signaling for cancer therapy. J Natl Cancer Inst 93:1062–1074

Arnold MR, Kremer W, Luedemann H-D, Kalbitzer HR (2002) ^{1}H NMR parameters of common amino acid residues measured in aqueous solutions of the linear tetrapeptides Gly-Gly-X-Ala at pressures between 0.1 and 200 MPa. Biophys Chem 96:129–140

Baines AT, Xu D, Der CJ (2011) Inhibition of Ras for cancer treatment: the search continues. Future Med Chem 3:1787–1808

Baskaran K, Brunner K, Munte CE, Kalbitzer HR (2010) Mapping of protein structural ensembles by chemical shifts. J Biomol NMR 48:71–83

Beck Erlach M, Koehler J, Moeser B, Horinek D, Kremer W, Kalbitzer HR (2014) Relationship between non-linear pressure induced chemical shift changes and thermodynamic parameters. J Chem Phys B 118:5681–5690

Bos JL (1989) Ras oncogenes in human cancer: a review. Cancer Res 49:4682–4689

Forsén S, Hoffman RA (1963) Study of moderately rapid chemical exchange reactions by means of nuclear magnetic double resonance. J Phys Chem 39:2892–2901

Friday BB, Adjei AA (2005) K-ras as a target for cancer therapy. Biochim Biophys Acta 1756:127–144

Geyer M, Schweins T, Herrmann C, Prisner T, Wittinghofer A, Kalbitzer HR (1996) Conformational transitions in p21ras and in its complexes with the effector protein raf-RBD and the GTPase activating protein GAP. Biochemistry 35:10302–10308

Heremans K, Smeller L (1998) Protein structure and dynamics at high pressure. Biochim Biophys Acta 1386:353–370

Herrmann C (2003) Ras-effector interactions: after one decade. Curr Opin Struct Biol 13:122–129

Iuga A, Spoerner M, Kalbitzer HR, Brunner E (2004) Solid-state 31P NMR spectroscopy of microcrystals of the Ras protein and its effector loop mutants: comparison of solution and crystal structures. J Mol Biol 342:1033–1040

Kalbitzer HR, Spoerner M (2013) State 1(T) inhibitors of activated Ras. In: Tamanoi F (ed) The enzymes, vol 33. Academic, Burlington, pp 69–94

Kalbitzer HR, Spoerner M, Ganser P, Hosza C, Kremer W (2009) Fundamental link between folding states and functional states of proteins. J Am Chem Soc 131:16714–16719

Kalbitzer HR, Rosnizeck IC, Munte CE, Puthenpurackal Narayanan S, Kropf V, Spoerner M (2013) Intrinsic allosteric inhibition of signaling proteins by targeting rare interaction states detected by high pressure NMR spectroscopy. Angew Chem Int Ed 52:14242–14246

Karnoub AE, Weinberg RA (2008) Ras oncogenes: split personalities. Mol Cell Biol 9:517–531

Koehler J, Beck Erlach M, Crusca E Jr, Kremer W, Munte CE, Kalbitzer HR (2012) On the pressure dependence of 15N chemical shifts in the model peptides Ac-Gly-Gly-X-Ala-NH2. Mater 5:1774–1786

Kremer W, Kachel N, Kuwata K, Akasaka K, Kalbitzer HR (2007) Species specific differences in the intermediate states of human and Syrian hamster prion protein detected by high pressure NMR spectroscopy. J Biol Chem 282:22689–22698

Long D, Marshall CB, Bouvignies G, Mazhab-Jafari MT, Smith MJ, Ikura M, Kay LE (2013) A comparative CEST NMR study of slow conformational dynamics of small GTPases complexed with GTP and GTP analogues. Angew Chem Int Ed 52:10107–10771

Loria JP, Rance M, Palmer AG (1999) A relaxation-compensated Carr-Purcell-Meiboom-Gill sequence for characterizing chemical exchange by NMR spectroscopy. J Am Chem Soc 121:2331–2332

Maurer T, Garrenton LS, Oh A, Keith P, Anderson DJ, Skelton NJ, Fauber BP, Pan B, Malek S, Stokoe D, Ludlam MJ, Bowman KK, Wu J, Giannetti AM, Starovasnik MA, Mellman I, Jackson PK, Rudolph J, Wang W, Fang G (2012) Small-molecule ligands bind to a distinct pocket in Ras and inhibit SOS-mediated nucleotide exchange activity. Proc Natl Acad Sci U S A 109:5299–5304

Monod J, Wyman J, Changeux JP (1965) On the nature of allosteric transitions: a plausible model. J Mol Biol 12:88–118

Neal S, Nip AM, Zhang H, Wishart DS (2003) Rapid and accurate calculation of protein ^{1}H, ^{13}C and ^{15}N chemical shifts. J Biomol NMR 2:215–240

O'Connor C, Kovrigin EL (2008) Global conformational dynamics in Ras. Biochemistry 47:10244–10246

Pai EF, Krengel U, Petsko GA, Goody RS, Kabsch W, Wittinghofer A (1990) Refined crystal structure of the triphosphate conformation of H-ras p21 at 1.35 a resolution: implications for the mechanism of GTP hydrolysis. EMBO J 9:2351–2359

Rajalingam K, Schreck R, Rapp UR, Albert S (2007) Ras oncogenes and their downstream targets. Biochim Biophys Acta 1773:1177–1195

Rosnizeck IC, Graf T, Spoerner M, Tränkle J, Filchtinski D, Herrmann C, Gremer L, Vetter IR, Wittinghofer A, König B, Kalbitzer HR (2010) Stabilizing a weak binding state for effectors in the human Ras-protein by cyclen complexes. Angew Chem Int Ed 49:3830–3833

Rosnizeck IC, Spoerner M, Harsch T, Kreitner S, Filchtinski D, Herrmann C, Engel D, König B, Kalbitzer HR (2012) Metal-bis(2-picolyl)amine complexes as state 1(T) inhibitors of activated Ras protein. Angew Chem Int Ed 51:10647–10651

Schöpel M, Jockers KFG, Düppe PM, Autzen J, Potheraveedu VN, Semra I, Yip KT, Heumann R, Herrmann C, Scherkenbeck J, Stoll R (2013) Bisphenol A binds to Ras proteins and competes with guanine nucleotide exchange: implications for GTPase-selective antagonists. J Med Chem 2013(56):9664–9672

Schumann FH, Riepl H, Maurer T, Gronwald W, Neidig K-P, Kalbitzer HR (2007) Combined chemical shift changes and amino acid specific chemical shift mapping of protein-protein interactions. J Biomol NMR 39:275–289

Spoerner M, Herrmann C, Vetter IR, Kalbitzer HR, Wittinghofer A (2001) Dynamic properties of the Ras switch I region and its importance for binding to effectors. Proc Natl Acad Sci U S A 98:4944–4949

Spoerner M, Wittinghofer A, Kalbitzer HR (2004) Perturbation of the conformational equilibria in Ras by selective mutations as studied by 31P NMR spectroscopy. FEBS Lett 578:305–310

Spoerner M, Nuehs A, Ganser P, Herrmann C, Wittinghofer A, Kalbitzer HR (2005a) Conformational states of Ras complexed with the GTP-analogs GppNHp or $GppCH_2p$: implications for the interaction with effector proteins. Biochemistry 44:2225–2236

Spoerner M, Graf T, König B, Kalbitzer HR (2005b) A novel mechanism for the modulation of the Ras-effector interaction by small molecules. Biochem Biophys Res Comm 334:709–713

Spoerner M, Nuehs A, Herrmann C, Steiner G, Kalbitzer HR (2007) Slow conformational dynamics of the guanine nucleotide-binding protein Ras complexed with the GTP analogue GTPγS. FEBS J 274:1419–1433

Spoerner M, Hozsa C, Poetzl JA, Reiss K, Ganser P, Geyer M, Kalbitzer HR (2010) Conformational states of rat sarcoma (Ras) protein complexed with its natural ligand GTP and their role for effector binding and GTP hydrolysis. J Biol Chem 285:39768–39778

Stumber M, Geyer M, Graf R, Kalbitzer HR, Scheffzek K, Haeberlen U (2002) Observation of slow dynamic exchange processes in Ras protein crystals by ^{31}P solid state NMR spectroscopy. J Mol Biol 323:899–907

Sun Q, Burke JP, Phan J, Burns MC, Olejniczak ET, Waterson AG, Lee T, Rossanese OW, Fesik SW (2012) Discovery of small molecules that bind to K-Ras and inhibit Sos-mediated activation. Angew Chem Int Ed 51:6140–6143

Wennerberg K, Rossman KL, Der CJ (2005) The Ras superfamily at a glance. J Cell Sci 118:843–846

Wittinghofer A, Waldmann H (2000) Ras-a molecular switch involved in tumor formation. Angew Chem Int Ed 39:4192–4214